Expression profile of microRNAs in fetal lung development of Sprague-Dawley rats

YANG YANG[1], GUO KAI[1], XIAO-DAN PU[2], KAN QING[2], XI-RONG GUO[3] and XIAO-YU ZHOU[2]

[1]Institute of Pediatrics, Nanjing Medical University, Nanjing 210029; [2]Department of Neonates, Nanjing Children's Hospital of Nanjing Medical University, Nanjing 210008; [3]Department of Pediatrics, Nanjing Maternal and Child Health Hospital of Nanjing Medical University, Nanjing 210004, P.R. China

Received October 9, 2011; Accepted November 14, 2011

DOI: 10.3892/ijmm.2011.855

Abstract. As well-known regulators of gene expression, microRNAs (miRNAs) play an important role not only in cell proliferation and differentiation, but also in tumorigenesis and organ development. Furthermore, it is estimated that miRNAs may be responsible for regulating the expression of nearly one-third of the human genome. Simultaneously, in the clinic, with advances in neonatal care, a larger number of premature infants are being saved, and thus diseases of lung development, including bronchopulmonary dysplasia (BPD) have become more and more common. However, only a few miRNA studies have studied their connection with diseases of lung development. In our study, we used a miRNA microarray including more than 1891 capture probes to profile the expression of miRNAs at three time points of rat lung development [embryonic (E) Day 16 (E16), E19, E21]. miRNAs found to have consistent fold-changes (fold-change>2.0) during all three time points were selected and validated by real-time PCR. As a result, 167 differentially expressed miRNAs were found during rat lung organogenesis, including 81 upregulated and 86 downregulated miRNAs. Seven miRNAs were selected and characterized by having a consistent >2-fold changes between all three groups. Among these 7 miRNAs, except for let-7a, the other 6 miRNAs (miR-1949, miR-125b-5p, miR-296, miR-93, miR-146b, miR-3560) are all first reported for the first time in lung development. Finally, due to the fact that they demonstrated higher fold changes, from these 7 miRNAs we selected miR-125b-5p, miR-296, miR-93, miR-146b and miR-3560 for real-time PCR. We hypothesized that these newly identified miRNAs may play an important role in fetal lung development, and this experimental result could help us to further clarify the mechanism of normal lung development including the development of type II pneumocytes. This may provide a physiological basis for future research on diseases of lung development.

Correspondence to: Dr Xiao-Yu Zhou, Department of Neonates, Nanjing Children's Hospital of Nanjing Medical University, 72 Guangzhou Road, Nanjing 210008, P.R. China
E-mail: xyzhou161@163.com

Key words: lung development, microRNA, SD rats, respiratory distress syndrome, bronchopulmonary dysplasia

Introduction

The discovery of miRNA is considered as one of the major science breakthroughs of the last several years. Different miRNAs are located in several different genomic locations, and because they can regulate the expression of mRNA, they are considered as important regulatory molecules that modulate various biological processes including cellular physiology, developmental timing, cell fate determination, insulin secretion, and progression of various cancers. Certainly, fetal lung development of mammals is also under the control of a complex network of miRNAs. In recent years, a number of miRNA profiling studies evaluating mouse and rat lung development have emerged, Williams *et al* (1) performed miRNA profiling at 3 time points (P1, P14 and P60) of the developing mouse lung and demonstrated that the overall expression profile of miRNAs was similar for mouse and human tissue. Bhaskaran *et al* (2) performed miRNA profiling at 7 time points in rat lung development and identified 21 miRNAs that showed significant changes in expression. Carraro *et al* (3) found that the mir-17 family of miRNA modulates FGF10-FGFR2b downstream signaling by specifically targeting STAT3 and MAPK14, hence further modulates epithelial bud morphogenesis of lungs in response to FGF10 signaling.

Though these related studies have reported the role of miRNAs in lung development, it's still necessary to re-screen miRNAs during the process of lung development based on three reasons. First of all, as a result of different research directions, researchers often select different time points of lung development and different screening criteria for miRNAs. Consequently, this will ultimately lead to distinct research significance, even if their research schemes are so similar. In addition, with great innovation of microarray technology and a quick increase of the probe sites, today's microarray contains more than 1891 capture probes, covering all human, mouse and rat miRNAs annotated in miRBase 16.0. Thence theoretically through these improved methods we could identify new miRNAs on lung development not identified before.

Nowadays, in the clinic, a larger number of premature infants are being saved, and as a result respiratory distress syndrome

(RDS) and bronchopulmonary dysplasia (BPD) have become more and more common. One widely accepted cause of BPD is immature fetal lung development in pregnancy and similarly, one known critical reason of RDS is secretion of insufficient pulmonary surfactant, which also occurs during fetal lung development. Thus, there should be a close link between these two neonatal diseases and the period of lung development. Besides, we have already known that lung development in the rat can be divided into five stages (4,5). In the first 13 days, this phase is the embryonic phase. During this stage lobar division takes place. The second phase is the pseudoglandular phase (13-18 days), in which epithelial tubes of air passages are formed. In the canalicular phase (18-20 days), lumens are divided into many tubules and the interstitium becomes thinner. Furthermore, lamellar bodies begin to emerge. At the saccular phase (20 days to full term), alveolar ducts and air sacs are formed. The final stage occurs after birth and is called the alveolar phase, in which true alveoli are formed. Among these stages, we chose the pseudoglandular, the canalicular and the saccular phases to represent the process of fetal lung development in our experiment.

Although the pathogenesis of the above two diseases has been studied widely before, there are few studies evaluating the links between BPD/RDS and miRNAs expression in fetal lung development. Zhang *et al* (6) reported that compared to the normal control, in the hyperoxia-exposed BPD group, 14 miRNAs were upregulated, and 7 miRNAs were down-regulated. This result further indicates that miRNAs might play an important role in the progress of BPD. Therefore, in light of the above three reasons, we finally chose three key time points [embryonic (E) Day 16 (E16), E19, E21] representing the process of normal fetal lung development to perform a new miRNAs screening, in an attempt to further explore the mechanism of fetal lung development and offer a physiological basis for the research of RDS and BPD in the future.

Materials and methods

Sprague-Dawley rats. All healthy adult rats (12 female rats and 12 male rats in total) were maintained in a specific-pathogen-free an animal facility at animal center of the Nanjing Medical University. All procedures in this study followed the protocols approved by the Nanjing Medical University Animal Care and Use Committee. Pregnant SD rats were sacrificed with CO_2, whole fetal lungs were immediately isolated from rats' fetuses on gestational Days 16, 19 and 21 (E16, E19, and E21), and these three time points were named as group S1(E21), group S2(E19), group S3(E16) respectively. For each group, there were 4 pregnant rats which were selected through a random contrast rule.

After isolation, lungs were washed with PBS. For each group one copy of fetal lungs was randomly kept for histological observation. Total-RNA of the left lungs was isolated using TRIzol (Invitrogen) and the miRNeasy mini kit (Qiagen) according to manufacturer's instructions. RNA quality and quantity was measured using the NanoDrop spectrophotometer (ND-1000, Nanodrop Technologies) and RNA integrity was determined by gel electrophoresis.

Histology. Paraformaldehyde-fixed lung tissue was paraffin embedded and 4 μm sections were obtained. Sections were stained with hematoxylin and eosin (H&E) for morphology detection. H&E sections were viewed with normal optical microscopy at x40 magnification for observing fetal lung development changes of the 3 groups (S1, S2, S3).

miRNA microarray. After RNA isolation from the fetal lungs, the miRCURY Hy3™/Hy5™ power labeling kit (Exiqon, Vedbaek, Denmark) was used according to the manufacturer's instractions for miRNA labeling. One microgram of each sample was 3'-end-labeled with Hy3™ fluorescent label, using T4 RNA ligase by the following procedure. RNA in 2.0 μl of water was combined with 1.0 μl of CIP buffer and CIP (Exiqon). The mixture was incubated for 30 min at 37˚C, and was terminated by incubation for 5 min at 95˚C. Then 3.0 μl of labeling buffer, 1.5 μl of fluorescent label (Hy3™), 2.0 μl of DMSO, 2.0 μl of labeling enzyme were added into the mixture. The labeling reaction was incubated for 1 h at 16˚C, and terminated by incubation for 15 min at 65˚C.

After terminating the labeling procedure, the Hy3™-labeled samples were hybridized on the miRCURY LNA™ array (v.16.0) (Exiqon) according to the manual. The total 25 μl mixture from Hy3™-labeled samples with of 25 μl hybridization buffer were first denatured for 2 min at 95˚C, incubated on ice for 2 min and then hybridized to the microarray for 16-20 h at 56˚C in a 12-Bay Hybridization system (Nimblegen Systems, Inc.; Madison, WI, USA), which provides an active mixing action and constant incubation temperature to improve hybridization uniformity and enhance the signal. Following hybridization, the slides were washed several times using wash buffer kit (Exiqon), and finally dried by centrifugation for 5 min at 400 rpm. Then the slides were scanned using the Axon GenePix 4000B microarray scanner (Axon Instruments, Foster City, CA, USA).

Scanned images were then imported into GenePix Pro 6.0 software (Axon) for grid alignment and data extraction. Replicated miRNAs were averaged and miRNAs that had intensities>50 in all samples were chosen for calculating the normalization factor. Expressed data were normalized using the median normalization. After normalization, differentially expressed miRNAs were identified through fold-change filtering (fold change>2.0). Hierarchical clustering was performed using the MEV software (v4.6, TIGR).

Quantitative real-time PCR. Total-RNA was isolated from fetal lungs using the TRIzol reagent (Invitrogen Life Technologies). Single-strand cDNA was synthesized as follows: the reverse transcription mixture contained 1 μg total-RNA, 0.3 μl rno-miRNA reverse primer (1 μM) (Table I), 0.1 μl MMLV revertase (200 U/μl, Epicentre), 2 μl 10X RT buffer, 2 μl dNTP mix (2.5 mM each), 0.3 μl ribonuclease inhibitor (40 U/μl, Epicentre), in a 20 μl total volume. The reaction was performed at 16˚C for 30 min and at 42˚C for 40 min, followed by heat inactivation at 85˚C for 5 min. For real-time PCR, 1 μl cDNA was added to 24 μl master mix containing 2.5 μl dNTP (2.5 mM each), 2.5 μl 10X PCR buffer (Promega), 1 unit Taq polymerase (Promega), final concentration 0.25X SYBR-Green I (Invitrogen) and 2 μl reverse and forward primers. cDNA was amplified for 35 cycles with the Applied Rotor-Gene 3000 (Corbett Research) real-time PCR system. The primer sequences used are listed

Table I. Reverse primer sequences.

Gene name	RT primers
U6	5'-CGCTTCACGAATTTGCGTGTCAT-3'
rno-miR-93	5'-GTCGTATCCAGTGCGTGTCGTGGAGTCGGCAATTGCACTGGATACGACCTACCTG-3'
rno-miR-125b-5p	5'-GTCGTATCCAGTGCGTGTCGTGGAGTCGGCAATTGCACTGGATACGACTCACAA-3'
rno-miR-146b	5'-GTCGTATCCAGTGCGTGTCGTGGAGTCGGCAATTGCACTGGATACGACACAGCCT-3'
rno-miR-3560	5'-GTCGTATCCAGTGCGTGTCGTGGAGTCGGCAATTGCACTGGATACGACAATGCAC-3'
rno-miR-296	5'-GTCGTATCCAGTGCGTGTCGTGGAGTCGGCAATTGCACTGGATACGACGGAGAG-3'

Table II. Primers for real-time RT-PCR.

Gene name		Primers	Ta (°C)
U6	F	5'-GCTTCGGCAGCACATATACTAAAAT-3'	
	R	5'-CGCTTCACGAATTTGCGTGTCAT-3'	60
rno-miR-93	GSP	5'-GGCAAAGTGCTGTTCGTG-3'	
	R	5'-CAGTGCGTGTCGTGGAGT-3'	60
rno-miR-125b-5p	GSP	5'-GGGTCCCTGAGACCCTAAC-3'	
	R	5'-CAGTGCGTGTCGTGGAGT-3'	60
rno-miR-146b	GSP	5'-GGGTGAGAACTGAATTCCAT-3'	
	R	5'-CAGTGCGTGTCGTGGAG-3'	60
rno-miR-3560	GSP	5'-GTCAAATCCTTGCCCG-3'	
	R	5'-CAGTGCGTGTCGTGGA-3'	60
rno-miR-296	GSP	5'-GAGGGTTGGGTGGAGG-3'	
	R	5'-CAGTGCGTGTCGTGGAG-3'	60

F, forward; R, reverse; GSP, gene-specific primer.

in Table II. RT and PCR for U6 snRNA were performed in each plate as an endogenous control. The amount of PCR product was calculated from the threshold cycle (Ct), and the comparative Ct method was used. The relative amount of each miRNA to U6 snRNA was calculated with the equation $2^{-(\text{Ct microRNA-Ct U6})}$.

Statistical analysis. Data were analyzed with the SPSS 13.0 statistical package, and the data of the real-time PCR was evaluated by one-way ANOVA. A P-value <0.05 was considered significant.

Results

Histology. In the S3(E16) group some epithelial tubes extending many branches like 'trees' were observed, which were all constructed of tall epithelial cells, arranged in irregular rings (Fig. 1C). In the S2(E19) group the bronchioles started to take shape. The interstitium was thinner than before and some gas chambers and primal alveolars appeared (Fig. 1B). In the S1(E21) group the alveolar structures expanded rapidly and the interstitium became more sparse than in the previous groups (Fig. 1A).

miRNA expression profile. We used the sixth generation of the miRCURY LNA Array (v.16.0) which contains more than 1891 capture probes, covering all human, mouse and rat miRNAs annotated in miRBase 16.0, as well as all viral miRNAs related to these species. In addition, this array also contains capture probes for 66 new miRPlus™ human miRNAs. As a result, through this microarray, 167 differentially expressed miRNAs between 3 groups (group S1, S2, S3) passed the fold-change filtering (fold-change >2.0), including 81 upregulated miRNAs and 86 downregulated miRNAs.

Among these differentially expressed miRNAs, we identified 40 downregulated and 37 upregulated miRNAs in S2/S3 (fold-change >2.0); 42 downregulated and 30 upregulated miRNAs in S1/S2 (fold-change >2.0); 50 downregulated and 48 upregulated miRNAs in S1/S3 (fold-change >2.0) (Tables V and VI). Then we performed hierarchical clustering to show distinguishable miRNA expression profiling among the groups. In the heat map diagram, each row represents a miRNA and each column represents a group. The miRNA clustering tree is shown on the left, and the group clustering tree appears at the top (Fig. 2).

From all the differentially expressed miRNAs (Tables V and VI) we set a specific criterion for screening miRNAs

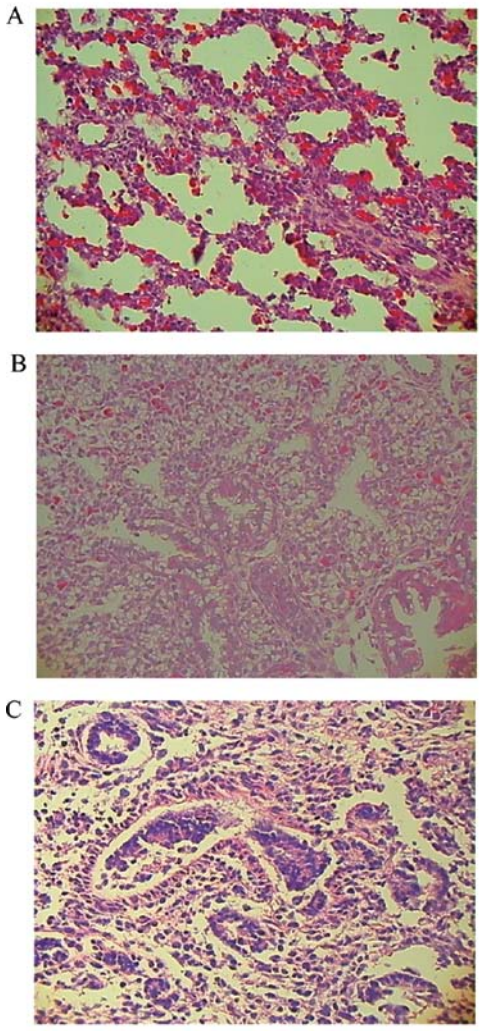

Figure 1. Observation of fetal lung tissue in 3 groups under as optical microscope, H&E, x40. (A-C) Representative photomicrographs of group S1(E21), S2(E19) and S3(E16), respectively.

we wished to further study. The screening criteria was that the expression of these miRNAs must meet the requirement of fold-changes in S2/S3>2.0 and S1/S2>2.0 and S1/S3>4.0 [S3(E16)→S2(E19)→S1(E21)]. After screening, we found 4 consistently downregulated and 3 consistently upregulated miRNAs that met our requirements between the 3 groups (Tables III and IV). The specific fold-changes of 4 downregulated and 3 upregulated miRNAs are compared using histograms (Fig. 3) based on the data of Tables III and IV. Besides this, the expression patterns of these identified miRNAs are also shown in the line charts (Fig. 4).

Because of showing more obvious fold-changes between 3 groups, at last, we further selected out 5 miRNAs based on the data of Fig. 3, including 3 downregulated miRNAs (miR-125b-5p, miR-296, miR-93) and 2 upregulated miRNAs (miR-146b, miR-3560).

Real-time PCR. These 5 selected miRNAs were confirmed by real-time PCR. We chose these 5 miRNAs for further study based on several reasons as follows. Firstly, among the 4 consistently downregulated miRNAs, miR-125b-5p, miR-296, miR-93 had greater fold-changes between the 3 groups than

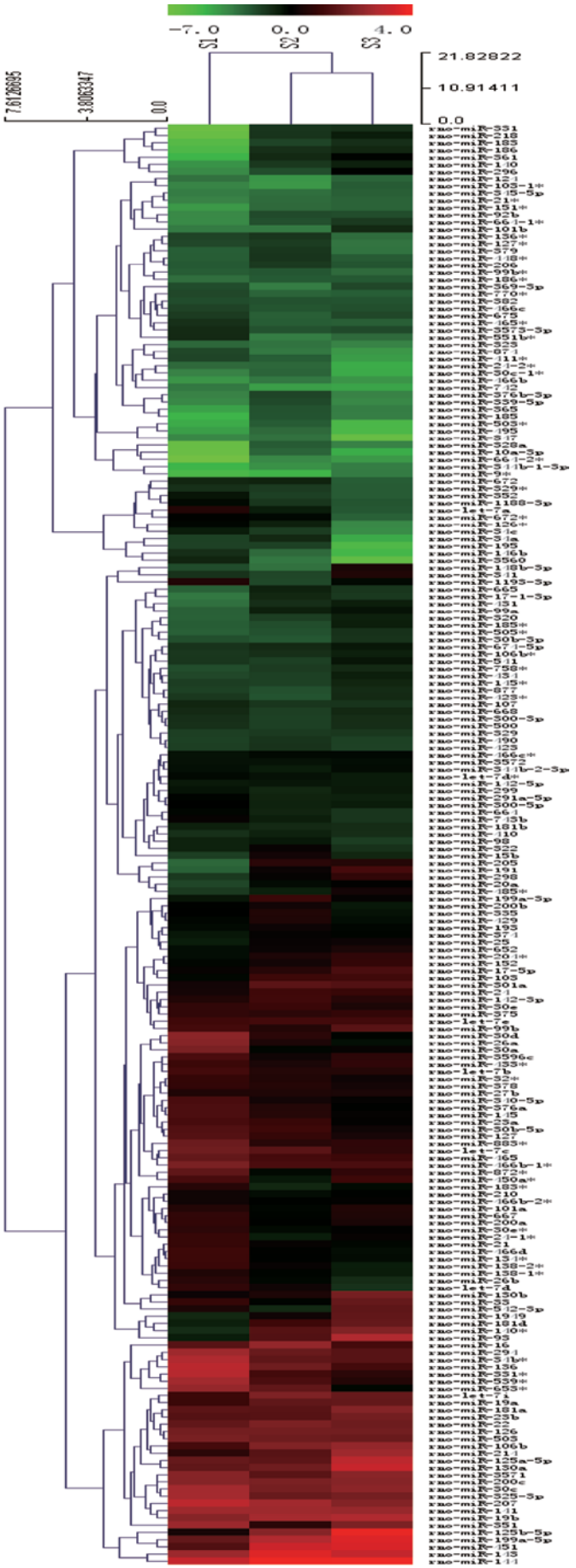

Figure 2. Hierarchical clustering of the 3 groups (S1, S2, S3). Distinguishable miRNA expression profiling is observed. Red indicates high relative expression, green indicates low relative expression and black represents zero.

Table III. Specific fold-changes of 4 consistently downregulated miRNAs after screening (S3→S2→S1 ↓).

	miR-125b-5p	miR-296	miR-93	miR-1949
S2/S3	0.350006	0.248001	0.359659	0.381056
S1/S2	0.273829	0.317061	0.242748	0.42356
S1/S3	0.095842	0.078631	0.087306	0.161400

Table IV. Specific fold-changes of 3 consistently upregulated miRNAs after screening (S3→S2→S1 ↑).

	miR-146b	miR-3560	let-7a
S2/S3	5.016317	8.421142	3.178521
S1/S2	3.094662	4.888906	2.289511
S1/S3	15.523805	41.170169	7.277257

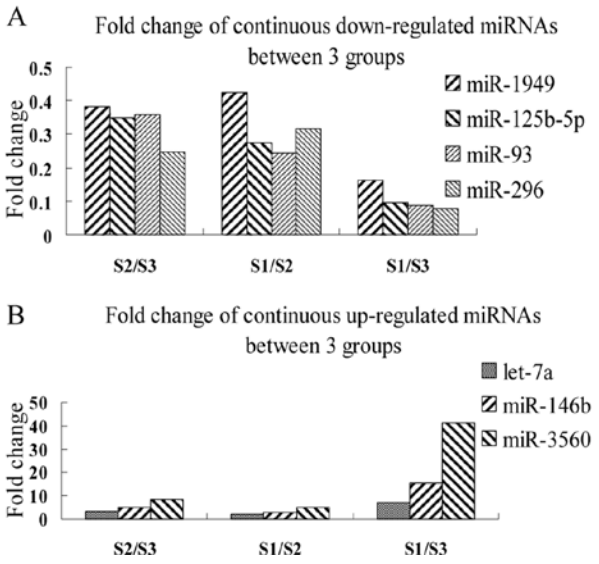

Figure 3. Comparison of specific fold-changes of 7 miRNAs. (A) The specific fold-changes of 4 consistently downregulated miRNAs between the 3 groups and (B) the specific fold-changes of 3 consistently upregulated miRNAs between the 3 groups.

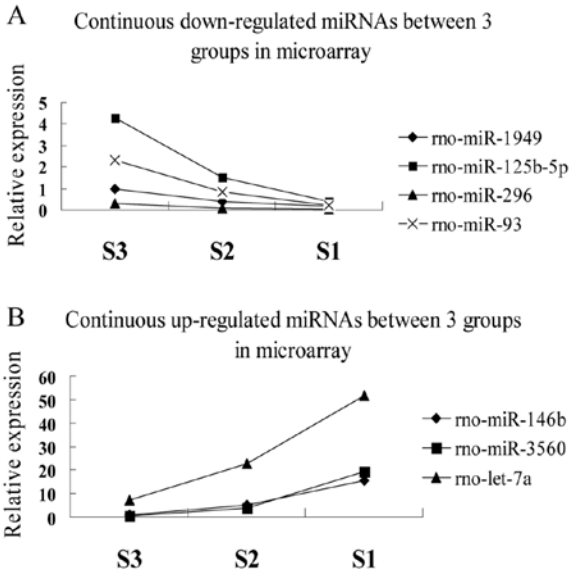

Figure 4. miRNA expression patterns during rat lung development. (A) The relative expression trend of 4 consistently downregulated miRNAs and (B) the relative expression trend of 3 consistently upregulated miRNAs after screening.

miR-1949. Similarly, among 3 consistently upregulated miRNAs, miR-146b, miR-3560 have greater fold changes between the 3 groups than let-7a (Fig. 3). Secondly, compared to the widely studied let-7a, we have known less about several other miRNAs. So finally we chose miR-125b-5p, miR-296, miR-93, miR-146b, miR-3560 to perform real-time PCR. The relative expressions of these 5 miRNAs are shown in Fig. 5.

Discussion

In our experiment, we found that miR-1949, miR-125b-5p, miR-296 and miR-93 were consistently downregulated, while miR-146b, miR-3560, let-7a were consistently upregulated between all three groups. Among them, miR-146b, miR-125b-5p, miR-1949 and miR-3560 are reported for the first time in lung development. Specifically for miR-1949 and miR-3560, there were no miRNAs studies involving them before. As for miR-296 and miR-93, they also have rarely been reported in lung development during previous studies.

Before our research, a series of studies had demonstrated the importance of miRNAs in the process of lung physiology. It was reported that miR-146 was upregulated in response to LPS, and negatively regulates the innate immune response (7). Hence the importance of miR-146b was mainly reflected in innate immune and inflammation response (7,8), but in lung development this is the first time it has been reported. Similarly, miR-125b-5p is also mainly related to the immune response (9). It was demonstrated that in response of LPS, miR-125b decreased by inhibition of κB-Ras2, an inhibitor of IκB (10). Androulidaki *et al* (11) further reported that both *in vitro* and *in vivo* suppression of miR-125b mainly depended on Akt signaling in murine macrophages. As for miR-93, from the report of Bhaskaran *et al* (2) miR-93 had a higher expression in E16 and declined with time in SD rat lung tissue. In addi-

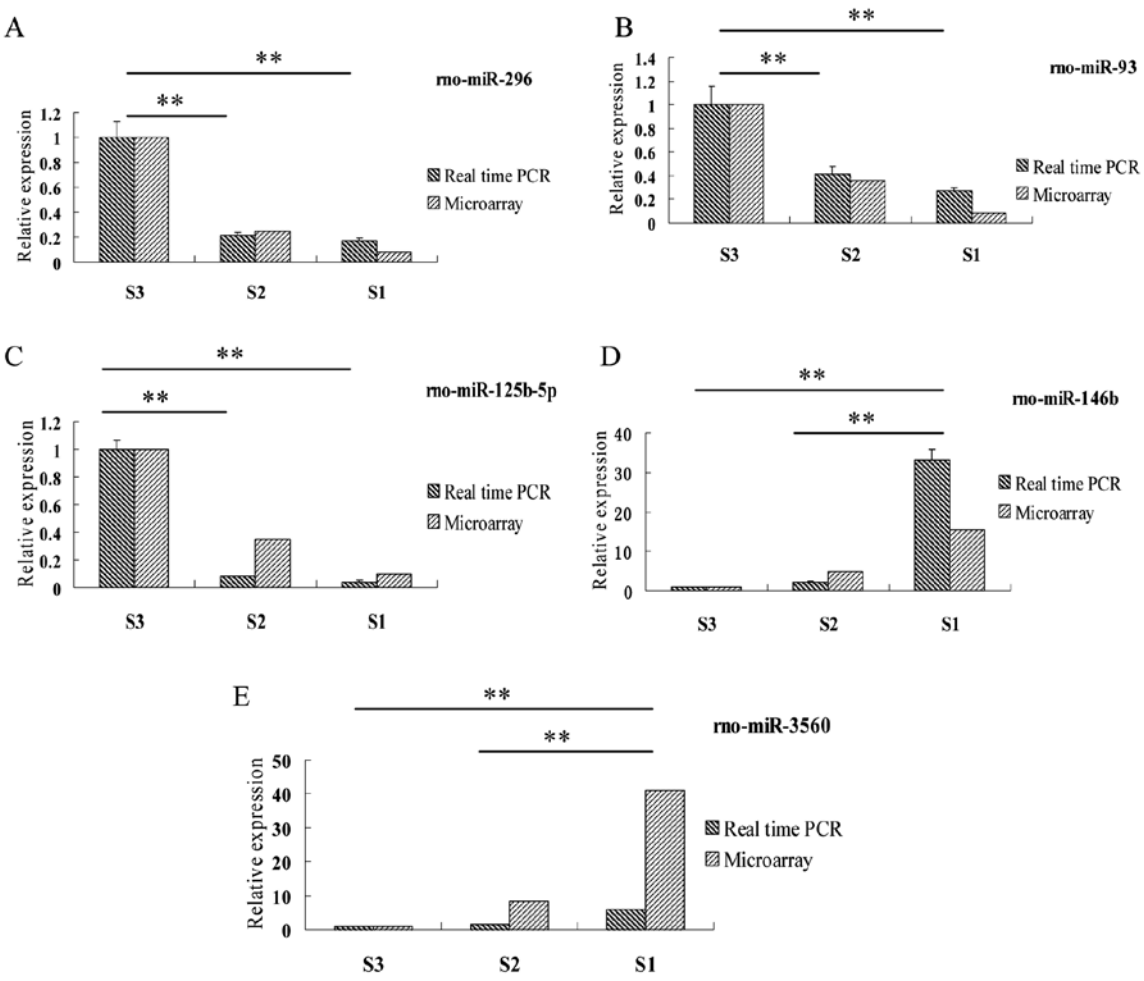

Figure 5. Validation of miRNA microarray results by real-time PCR. Triplicate assays were performed from each RNA sample. Data are normalized using U6 as an endogenous control for RNA input. Fold changes for these miRNAs from array and real-time qRT-PCR are shown as the mean. Error bars represent SE. All exhibited statistical significance of real-time PCR was tested by the one-way ANOVA test (**P<0.001).

tion, Foshay and Gallicano (12) demonstrated that miR-93 and several other miRNAs are differentially expressed in developing mouse embryos and function to control differentiation of stem cells. Besides, Long *et al* (13) provided evidence that miR-93 regulates VEGF expression in experimental models of diabetes both *in vitro* and *in vivo*. Anti-miR-93 inhibitors increased VEGF release. These findings show that miR-93 plays an important role in early organ development including lung tissue, and maybe it promotes organ development via its role in regulating VEGF expression and differentiation of stem cells. Another mentioned microRNA, miR-296, was found having high expression both in mouse and human fetal lung development (1). Besides, Würdinger *et al* (14) further demonstrated that miR-296 has a major role in the upregulation of growth factor receptors on endothelial cells during angiogenesis. These facts also show the function of miR-296 in organ growth and development.

Among all those miRNAs on lung development, without no doubt the let-7 family and the miR-17-92 cluster have been studied the most. As for the let-7 family, this is the first reported miRNA family in humans (15). Important known targets of let-7 are the mRNAs for Ras proteins (16). Ras proteins lie downstream of receptor tyrosine kinase signaling, including the fibroblast growth factor (FGF) receptors. FGF signaling is known to be important for lung branching morphogenesis and epithelial cell proliferation (17-19). Hence the let-7 family would be highly expressed and should play an important part in normal neonatal lung development. In addition, Chen *et al* (20) showed that in the immune response the presence of LPS, let-7i expression is reduced in a MyD88/NF-κB-dependent manner accompanied by a concomitant increase in TLR4 protein. They found that let-7b and let-7g are also predicted to target TLR4 (20). These findings suggest that the let-7 family is essential in the normal immune system of the lungs as well. Beside its roles in these aspects, the let-7 family also plays an important role in the domain of lung cancer because of the ability of modulating proliferation and differentiation. *In vitro*, Johnson *et al* (21) showed that let-7 is highly expressed in normal lung tissue, and can repress cell proliferation pathways. Moreover, overexpression of let-7 in cancer cell lines alters cell cycle progression and reduces cell division, providing evidence that let-7 functions as a tumor suppressor in normal lung cells (21). This observation also further supported the links between let-7 and cell proliferation of lungs. In our experiment, we identified several members of the let-7 family as well, such as let-7a, let-7d, let-7c, let-7i (Tables V and VI). In addition, we found that let-7a was consistently upregulated exhibiting more than 2-fold changes between all three groups. From the above

Table V. Differentially expressed downregulated miRNAs of the 3 groups.

S2 vs. S3[a]		S1 vs. S3[a]		S1 vs. S2[a]	
rno-miR-148b-3p	0.094091722	rno-miR-218	0.017748926	rno-miR-331	0.025097528
rno-miR-181c*	0.102332859	rno-miR-331	0.022676474	rno-miR-218	0.029062058
rno-miR-181a-2*	0.102496854	rno-miR-361	0.035607027	rno-miR-186	0.054194422
rno-miR-708	0.158107968	rno-miR-183	0.043789053	rno-miR-328a	0.059769138
rno-miR-542-3p	0.168129140	rno-miR-186	0.044599141	rno-miR-10a-3p	0.066155885
rno-miR-345-3p	0.185715189	rno-miR-191	0.074433158	rno-miR-183	0.067858632
rno-miR-341	0.194309188	rno-miR-296	0.078631409	rno-miR-361	0.068270782
rno-miR-872	0.198980560	rno-miR-93	0.087306489	rno-miR-664-2*	0.087026492
rno-miR-101b	0.221089511	rno-miR-125b-5p	0.095841547	rno-miR-205	0.096042750
rno-miR-675*	0.222038393	rno-miR-205	0.102436107	rno-miR-191	0.146809908
rno-miR-100	0.230750565	rno-miR-140*	0.105805164	rno-miR-185	0.157339286
rno-miR-296	0.248000552	rno-miR-140	0.107083030	rno-miR-140*	0.172848464
rno-miR-221*	0.269476529	rno-miR-328a	0.122790295	rno-miR-140	0.177829281
rno-miR-33	0.293467319	rno-miR-1949	0.161399938	rno-miR-365	0.214306279
rno-miR-1193-3p	0.299534761	rno-miR-181d	0.188473763	rno-miR-503*	0.216390196
rno-miR-9*	0.304562081	rno-miR-148b-3p	0.189087830	rno-miR-17-1-3p	0.216487388
rno-miR-103-1*	0.318368895	rno-miR-431	0.202831654	rno-miR-93	0.242748162
rno-miR-301b	0.341714335	rno-miR-298	0.203989814	rno-miR-146a	0.249292025
rno-miR-125a-5p	0.346604792	rno-miR-101b	0.209897940	rno-miR-451	0.253399034
rno-miR-125b-5p	0.350005640	rno-miR-664-1*	0.219644982	rno-miR-15b	0.257022296
rno-miR-130b	0.353168958	rno-miR-451	0.222592972	rno-miR-125b-5p	0.273828579
rno-miR-324-5p	0.357412560	rno-miR-99a	0.225967175	rno-miR-99a	0.287610683
rno-miR-31	0.357860445	rno-miR-9*	0.239133724	rno-miR-665	0.291447536
rno-miR-93	0.359658704	rno-miR-199a-5p	0.263862490	rno-miR-431	0.293607410
rno-miR-130a	0.374817120	rno-miR-20a	0.265100100	rno-miR-181d	0.304485508
rno-miR-369-3p	0.378716327	rno-miR-214	0.266488970	rno-miR-339-5p	0.312144607
rno-miR-1949	0.381055611	rno-miR-485*	0.281452769	rno-miR-92b	0.314976564
rno-miR-351	0.383714084	rno-miR-341	0.282151269	rno-miR-296	0.317061429
rno-miR-185*	0.385377368	rno-miR-185*	0.286100018	rno-miR-376b-3p	0.320623917
rno-miR-124	0.390480647	rno-miR-320	0.286974485	rno-miR-298	0.327527708
rno-miR-10a-5p	0.406082775	rno-miR-130b	0.297653142	rno-miR-664-1*	0.334675953
rno-miR-541	0.425408962	rno-miR-17-1-3p	0.314625186	rno-miR-20a	0.335312329
rno-miR-3568	0.431586754	rno-miR-130a	0.316640012	rno-miR-495	0.350653084
rno-miR-423*	0.440840707	rno-miR-92b	0.323796325	rno-miR-199a-3p	0.381904552
rno-miR-214	0.451194456	rno-miR-344b-1-3p	0.337673310	rno-miR-151*	0.394178815
rno-let-7a-2*	0.471572424	rno-miR-185	0.340510901	rno-miR-1949	0.423560063
rno-miR-103	0.477689243	rno-miR-151*	0.351659779	rno-miR-199a-5p	0.425979254
rno-miR-125a-3p	0.485123886	rno-miR-125a-5p	0.385950379	rno-miR-301a	0.428990949
rno-miR-877	0.486867326	rno-miR-106b	0.416344581	rno-let-7i	0.460781156
rno-miR-485*	0.498217593	rno-miR-505*	0.417283916	rno-miR-448*	0.474806300
		rno-miR-103	0.429258011	rno-miR-379	0.476652731
		rno-miR-434	0.437993715	rno-miR-143	0.485784973
		rno-miR-665	0.444955831		
		rno-miR-542-3p	0.450829869		
		rno-miR-17-5p	0.463810796		
		rno-miR-103-1*	0.466393222		
		rno-miR-365	0.467547660		
		rno-miR-301a	0.468096601		
		rno-miR-204*	0.469731276		
		rno-miR-758*	0.494091963		

[a]Two-fold downregulated miRNAs (arranged from high to low).

Table VI. Differentially expressed upregulated miRNAs of the 3 groups.

S2 vs. S3[a]		S1 vs. S3[a]		S1 vs. S2[a]	
rno-miR-328b-3p	55.43029872	rno-miR-3560	41.17016898	rno-miR-1193-3p	5.522615564
rno-miR-34b	25.20420420	rno-miR-146b	15.52380467	rno-miR-3560	4.888905952
rno-miR-195	13.54962858	rno-miR-195	13.35300725	rno-miR-551b*	4.873483536
rno-miR-34a	12.42613290	rno-miR-340-3p	11.43789966	rno-miR-3596b	4.612404060
rno-miR-347	10.65967283	rno-miR-126*	11.37482850	rno-miR-30a	4.448185340
rno-miR-3560	8.421141536	rno-miR-34c	8.819649047	rno-miR-351	3.656196612
rno-miR-126*	7.523952406	rno-miR-34a	7.506207336	rno-miR-331*	3.647136410
rno-miR-503*	7.362280702	rno-let-7a	7.277256972	rno-miR-872*	3.472207096
rno-miR-495	6.028228773	rno-miR-672*	6.182533418	rno-miR-26a	3.452368618
rno-miR-672*	5.260179147	rno-miR-653*	6.113379807	rno-miR-450a*	3.284467450
rno-miR-146b	5.016316626	rno-miR-26a	5.940862902	rno-miR-146b	3.094662045
rno-miR-34c	4.506134424	rno-miR-30d	5.322979658	rno-miR-30d	3.044324090
rno-miR-10a-3p	4.097022079	rno-miR-411*	5.276145472	rno-miR-183*	2.938326520
rno-miR-30c-1*	3.880991088	rno-miR-331*	4.862644551	rno-miR-24-1*	2.889240932
rno-miR-24-2*	3.864698405	rno-miR-874	4.551089902	rno-miR-542-3p	2.681449923
rno-miR-150	3.671263592	rno-miR-539*	4.305674923	rno-miR-539*	2.621550834
rno-miR-653*	3.464938036	rno-let-7d	4.232003213	rno-miR-34b*	2.423233055
rno-miR-411*	3.317823169	rno-miR-1188-3p	4.122995241	rno-miR-874	2.413460795
rno-miR-339-5p	3.191308237	rno-miR-352	3.863046748	rno-miR-369-3p	2.411181539
rno-let-7a	3.178520626	rno-miR-136	3.779750375	rno-miR-352	2.337056877
rno-miR-379	3.124849546	rno-miR-30a	3.710021556	rno-miR-136	2.305536320
rno-miR-672	3.073862020	rno-miR-24-2*	3.669641211	rno-miR-1188-3p	2.298812988
rno-miR-376b-3p	3.065376187	rno-miR-551b*	3.447018045	rno-miR-465*	2.298723191
rno-let-7d	2.913643907	rno-miR-26b	3.337770797	rno-let-7a	2.289510696
rno-miR-136*	2.806401138	rno-miR-138-2*	3.024870130	rno-miR-883*	2.217677800
rno-miR-127*	2.788147050	rno-miR-743b	2.893691660	rno-miR-3573-3p	2.199396790
rno-miR-322	2.718108021	rno-miR-672	2.876126516	rno-miR-742	2.165992682
rno-miR-16	2.412443817	rno-miR-34b*	2.644856632	rno-miR-134*	2.038410918
rno-miR-15b	2.290078069	rno-miR-742	2.462802491	rno-miR-124	2.030618140
rno-miR-433	2.184634072	rno-miR-465*	2.401121956	rno-miR-148b-3p	2.009611745
rno-miR-365	2.181679706	rno-miR-664	2.385839913		
rno-miR-185	2.164182316	rno-miR-376a	2.356517858		
rno-miR-542-5p	2.159287689	rno-miR-134*	2.348356145		
rno-miR-222	2.149338114	rno-miR-30c-1*	2.290029357		
rno-miR-98	2.148547043	rno-miR-127*	2.276946053		
rno-miR-328a	2.054409673	rno-miR-450a*	2.272963605		
rno-miR-448*	2.052694520	rno-miR-329*	2.244228769		
		rno-miR-145	2.236167326		
		rno-miR-294	2.190704795		
		rno-miR-138-1*	2.167812378		
		rno-miR-30b-5p	2.162192845		
		rno-miR-340-5p	2.148757049		
		rno-miR-23a	2.147419285		
		rno-let-7c	2.146358153		
		rno-miR-136*	2.071692663		
		rno-miR-127	2.065187461		
		rno-miR-21	2.060560052		
		rno-miR-883*	2.053969554		

[a]Two-fold upregulated miRNAs (arranged from high to low).

we could see that the let-7 family plays an indispensable role in normal lung development and homeostasis.

Except for the let-7 family just discussed, the expression of the miR-17-92 cluster is also high in embryonic development. Its expression declines steadily through development (22). Ventura *et al* (23) demonstrated that mice deficient in the miR-17-92 cluster exhibit lung hypoplasia defects characterized by smaller size, hypoplasia of the lung, ventricular septal defects, and by abnormal B-cell development. On the other hand, the overexpression of the miR-17-92 cluster in murine models resulted in an abnormal phenotype manifested by absence of terminal air sacs, which were replaced with highly proliferative, undifferentiated epithelium (22). In our research, we also found some members, such as miR-20a, miR-17-5p, miR-17-1-3p (Tables V and VI), they were downregulated in at least one pair of the 3 groups. However, due to the fact that the expression of the miR-17-92 cluster declines rapidly through the process of lung development, members that were consistently downregulated exhibiting more than 2-fold change between all three groups were not identified.

Apart from the above miRNAs discussed, we also found other ones reported in previous studies on lung development, such as miR-298, miR-146a, miR-199a, miR-127, miR-15b, miR-16, miR-26a (Tables V and VI). Due to space constraints of this manuscript, we will not discuss them. These several miRNAs all showed significant fold changes, but interestingly they did not show fold-changes between all three groups. We hypothesize that the reason is related to our strict screening criteria for microarray, requesting consistent >2-fold changes between all three groups.

In the clinic, advancements in neonatal techniques have improved the prognosis of preterm infants, and the followed incidence of BPD and RDS also gradually increases. Though there have not been accurate statistics of a large sample study in China, in America, the incidence of BPD has risen to about 3,000-7,000 birth per year (24). Currently, most researchers believe that BPD is a sophisticated networked disease caused by many factors. Although a new definition for BPD has been developed (25), the essence of this disease has already widely been agreed on, namely that it is a lung injury led by various risk factors including oxygen toxicity, mechanical ventilation, infection and inflammation on the basis of genetic susceptibility (25,26). Besides these factors, it has also been reported both in China and abroad that the incidence of BPD gradually increases with gestational age and birth-weight decreases (24,27). These findings show that the immature development of the fetal lungs is a key of the pathogenesis of BPD. In premature infants, because of lower numbers and a simpler structure of alveolars, the whole process of lung development has not yet been fulfilled. Then in the wake of being affected by different risk factors, it will finally lead to lung injury and a developmental lag.

Besides BPD, RDS is another common disease in newborns. Nowadays, it has already been proven that lack of alveolar surfactant is an important cause of RDS in the process of lung development. Simultaneously, it has been reported that the occurrence of RDS is also closely-related to gestational age and birth-weight during late pregnancy (28,29). We therefore, speculated whether the lungs would develop more completely with increased gestational age and birth-weight. This leads to a lower incidence of RDS along with an increase of secreting alveolar surfactant.

In conclusion, our experiments identified several consistently differentially expressed miRNAs between all three groups in fetal lung development. These results support the notion that to some degree these newly found miRNAs play a role in lung development, and we think it may help us to clarify the mechanism of normal lung development including the development type II pneumocytes, which may further provide a physiological basis for future research on RDS and BPD.

Acknowledgements

This study was supported by grants from the Project Foundation of Jiangsu Province Health Department (no. H200642). We thank Mrs. Jie Qiu for his assistance with the manuscript.

References

1. Williams AE, Moschos SA, Perry MM, Barnes PJ and Lindsay MA: Maternally imprinted microRNAs are differentially expressed during mouse and human lung development. Dev Dyn 236: 572-580, 2007.
2. Bhaskaran M, Wang Y, Zhang H, Weng T, Baviskar P, Guo Y, Gou D and Liu L: MicroRNA-127 modulates fetal lung development. Physiol Genomics 37: 268-278, 2009.
3. Carraro G, El-Hashash A, Guidolin D, Tiozzo C, Turcatel G, Young BM, De Langhe SP, Bellusci S, Shi W, Parnigotto PP and Warburton D: miR-17 family of microRNAs controls FGF10-mediated embryonic lung epithelial branching morphogenesis through MAPK14 and STAT3 regulation of E-Cadherin distribution. Dev Biol 333: 238-250, 2009.
4. Burri PH: Fetal and postnatal development of the lung. Annu Rev Physiol 46: 617-628, 1984.
5. Zoetis T and Hurtt ME: Species comparison of lung development. Birth Defects Res B Dev Reprod Toxicol 68: 121-124, 2003.
6. Zhang X, Peng W, Zhang S, Wang C, He X, Zhang Z, Zhu L, Wang Y and Feng Z: MicroRNA expression profile in hyperoxia-exposed newborn mice during the development of bronchopulmonary dysplasia. Respir Care 56: 1009-1015, 2011.
7. Taganov KD, Boldin MP, Chang KJ and Baltimore D: NF-kappaB-dependent induction of microRNA miR-146, an inhibitor targeted to signaling proteins of innate immune responses. Proc Natl Acad Sci USA 103:12481-12486, 2006.
8. Perry MM, Williams AE, Tsitsiou E, Larner-Svensson HM and Lindsay MA: Divergent intracellular pathways regulate interleukin-1beta-induced miR-146a and miR-146b expression and chemokine release in human alveolar epithelial cells. FEBS Lett 583: 3349-3355, 2009.
9. Tili E, Michaille JJ, Cimino A, Costinean S, Dumitru CD, Adair B, Fabbri M, Alder H, Liu CG, Calin GA and Croce CM: Modulation of miR-155 and miR-125b levels following lipopolysaccharide/TNF-alpha stimulation and their possible roles in regulating the response to endotoxin shock. J Immunol 179: 5082-5089, 2007.
10. Murphy AJ, Guyre PM and Pioli PA: Estradiol suppresses NF-kappaB activation through coordinated regulation of let-7a and miR-125b in primary human macrophages. J Immunol 184: 5029-5037, 2010.
11. Androulidaki A, Iliopoulos D, Arranz A, Doxaki C, Schworer S, Zacharioudaki V, Margioris AN, Tsichlis PN and Tsatsanis C: The kinase Akt1 controls macrophage response to lipopolysaccharide by regulating microRNAs. Immunity 31: 220-231, 2009.
12. Foshay KM and Gallicano GI: miR-17 family miRNAs are expressed during early mammalian development and regulate stem cell differentiation. Dev Biol 326: 431-443, 2009.
13. Long J, Wang Y, Wang W, Chang BH and Danesh FR: Identification of microRNA-93 as a novel regulator of vascular endothelial growth factor in hyperglycemic conditions. J Biol Chem 285: 23457-23465, 2010.
14. Würdinger T, Tannous BA, Saydam O, Skog J, Grau S, Soutschek J, Weissleder R, Breakefield XO and Krichevsky AM: miR-296 regulates growth factor receptor overexpression in angiogenic endothelial cells. Cancer Cell 14: 382-393, 2008.

15. Hutvágner G, McLachlan J, Pasquinelli AE, Bálint E, Tuschl T and Zamore PD: A cellular function for the RNA-interference enzyme Dicer in the maturation of the let-7 small temporal RNA. Science 293: 834-838, 2001.
16. Johnson SM, Grosshans H, Shingara J, Byrom M, Jarvis R, Cheng A, Labourier E, Reinert KL, Brown D and Slack FJ: Ras is regulated by the let-7 microRNA family. Cell 120: 635-647, 2005.
17. Cardoso WV and Lu J: Regulation of early lung morphogenesis: questions facts and controversies. Development 133: 1611-1624, 2006.
18. White AC, Xu J, Yin Y, Smith C, Schmid G and Ornitz DM: Fgf9 and Shh signaling coordinate lung growth and development through regulation of distinct mesenchymal domains. Development 133: 1507-1517, 2006.
19. Ramasamy SK, Mailleux AA, Gupte VV, Mata F, Sala FG, Veltmaat JM, Del Moral PM, De Langhe S, Parsa S, Kelly LK, Kelly R, Shia W, Keshet E, Minoo P, Warburton D and Bellusci S: Fgf10 dosage is critical for the amplification of epithelial cell progenitors and for the formation of multiple mesenchymal lineages during lung development. Dev Biol 307: 237-247, 2007.
20. Chen XM, Splinter PL, O'Hara SP and LaRusso NF: A cellular micro-RNA, let-7i, regulates Toll-like receptor 4 expression and contributes to cholangiocyte immune responses against *Cryptosporidium parvum* infection. J Biol Chem 282: 28929-28938, 2007.
21. Johnson CD, Esquela-Kerscher A, Stefani G, Byrom M, Kelnar K, Ovcharenko D, Wilson M, Wang X, Shelton J, Shingara J, Chin L, Brown D and Slack FJ: The let-7 microRNA represses cell proliferation pathways in human cells. Cancer Res 67: 7713-7722, 2007.
22. Lu Y, Thomson JM, Wong HY, Hammond SM and Hogan BL: Transgenic overexpression of the microRNA miR-17-92 cluster promotes proliferation and inhibits differentiation of lung epithelial progenitor cells. Dev Biol 310: 442-453, 2007.
23. Ventura A, Young AG, Winslow MM, Lintault L, Meissner A, Erkeland SJ, Newman J, Bronson RT, Crowley D, Stone JR, Jaenisch R, Sharp PA and Jacks T: Targeted deletion reveals essential and overlapping functions of the miR-17 through 92 family of miRNA clusters. Cell 132: 875-886, 2008.
24. Monte LF, Silva Filho LV, Miyoshi MH and Rozov T: Bronchopulmonary dysplasia. J Pediatr (Rio J) 81: 99-110, 2005 (In Portuguese).
25. Jobe AH and Bancalari E: Bronchopulmonary dysplasia. Am J Respir Crit Care Med 163: 1723-1729, 2001.
26. Coalson JJ: Pathology of new bronchopulmonary dysplasia. Semin Neonatol 8: 73-81, 2003.
27. Yu JQ, Zhang ZM, Zhang XY, Liu J and Feng ZC: An analysis of risk factors of premature infants with bronchopulmonary dysplasia. Chin Woman Child Health Res 3: 261-263, 2010.
28. Dani C, Reali MF, Bertini G, Wiechmann L, Spagnolo A, Tangucci M and Rubaltelli FF: Risk factors for the development of respiratory distress syndrome and transient tachypnoea in newborn infants. Eur Respir J 14: 155-159, 1999.
29. Qian LL, Liu CQ, Guo YX, Jiang YJ, Ni LM, Xia SW, Liu XH, Zhuang WZ, Xiao ZH, Wang SN, Zhou XY and Sun B: Current status of neonatal acute respiratory disorders: a one-year prospective survey from a Chinese neonatal network. Chin Med J (Engl) 123: 2769-2775, 2010.